

# Electrokinetic Propulsion of Polymer Microparticulates Along Glassy Carbon Electrode Array

#### **Jennifer Cortez**

Department of Biomedical Engineering, University of California, Irvine, Irvine, CA 92697-3975

## Kimia Damyar

Department of Biological Sciences, University of California, Irvine, Irvine, CA 92697-3975

#### **Runtian Gao**

College of Chemistry and Chemical Engineering, Xiamen University, Xiamen, Fujian 361005, China

#### Tuo Zhou

Materials and Manufacturing Technology, University of California, Irvine, Irvine, CA 92697-3975

# Lawrence Kulinsky<sup>1</sup>

Department of Mechanical and Aerospace Engineering, University of California, Irvine, Irvine, CA 92697-3975

e-mail: lkulinsk@uci.edu

Dielectrophoresis (DEP) is a force applied to microparticles in nonuniform electric field. This study discusses the fabrication of the glassy carbon interdigitated microelectrode arrays using lithography process based on lithographic patterning and subsequent pyrolysis of negative SU-8 photoresist. Resulting highresistance electrodes would have the regions of high electric field at the ends of microarray as demonstrated by simulation. The study demonstrates that combining the alternating current (AC) applied bias with the direct current (DC) offset allows the user to separate subpopulations of microparticulates and control the propulsion of microparticles to the high field areas such as the ends of the electrode array. The direction of the movement of the particles can be switched by changing the offset. The demonstrated novel integrated DEP separation and propulsion can be applied to various fields including in vitro diagnostics as well as to microassembly technologies. [DOI: 10.1115/1.4046561]

Keywords: microassembly, electrokinetic assembly, microparticles, dielectrophoresis, carbon electrodes

#### 1 Introduction

Electrokinetic propulsion can be utilized in a wide variety of applications, including lab-on-chip devices as well as for microassembly [1,2]. Direct and indirect fluidic manipulation of particles can be driven by induced charge electrokinetic phenomena, electrophoresis, electro-osmosis, dielectrophoresis (DEP), and electrothermal flows [3]. In conventional DEP, the transportation of

microparts can be controlled by the geometry of the electrodes and channels, particle size, and material.

Dielectrophoresis is the movement of dielectric particles in a nonuniform electric field. It transports particles toward the positions of the highest electric field gradient and can be either attractive—so-called positive DEP (pDEP) or repulsive—termed the negative DEP (nDEP). Whether the DEP force is positive or negative depends on the sign of Claussius—Mossotti factor K, as shown in the following equation:

$$K = \frac{\epsilon_{\rm p}^* - \epsilon_{\rm m}^*}{\epsilon_{\rm p}^* + 2\epsilon_{\rm m}^*} \tag{1}$$

where  $\varepsilon_i^*$  stands for complex permittivity of the materials and subscripts p and m identify particles and suspension media, respectively [4].

Dielectrophoretic force, given by Eq. (2), depends on the particle radius, R, the real part of the Claussius–Mossotti factor Re [K], and the gradient of the square of the electric field E

$$F_{\rm DEP} = 2\pi\epsilon_{\rm m}R^3{\rm Re}[K](\nabla E^2)$$
 (2)

Attractive and repulsive forces cause particles to be trapped in or move between the zones of high or low electric field. In an interdigitated electrode array (IDEA), there are two sites having the strongest gradient of the electric field: the pits along the length of electrodes and the ends of the electrodes.

This study looks at the propulsion of the polystyrene microbeads under the various electrical alternating current (AC) bias applied to the IDEAs of carbon microelectrodes. We describe a novel phenomenon—a dielectrophoretic propulsion that takes place along the length of the interdigitated electrode, whereas the classically expected DEP movement is just the attraction or repulsion toward or away from the adjacent electrodes. Because the beads used in this study are nonionic and do not natively have excess charges, the described phenomenon cannot be explained by the electro-osmosis and thus do not belong to the variety of the described electrokinetic propulsion methods [5]. We propose that the reason the beads move along the length of the electrodes is due to the fact that the beads move toward the region of high electric field that is located at the tip of the electrodes as demonstrated by the finite element analysis simulation described in Sec. 3. We also demonstrate that in high-resistance interdigitated electrode system, attractive and repulsive DEP in the transverse direction (i.e., toward or away from the adjacent electrodes) would act nearly identical to that of metal electrodes as the equivalent electrical circuit of the IDEA system will be dominated by much higher resistance of the liquid channel between the electrodes.

The longitudinal DEP propulsion can provide a noncontact force under which particles can be directed toward the sites of strongest electric field, and when coupled with pDEP or nDEP in transverse direction, it can be utilized as a guided microassembly tool by noncontact forces for integrated separation, sorting, and agglomeration of microparts. One of the possible applications demonstrated in this study is the combination of the separation of one type of beads (5  $\mu$ m diameter polystyrene beads) from heterogeneous suspension of 1 and 5  $\mu$ m diameter beads and removal of 5  $\mu$ m beads only by propelling these beads to one side of the electrode array.

#### 2 Materials and Methods

**2.1 Fabrication.** For fabrication of interdigitated electrodes, a 100-mm diameter single-crystal Si (001) wafer with 10,000-A thick silicon dioxide was used as a substrate for the fabrication of IDEAs. The electrode design schematics and the micrograph of the IDEAs used in this work is presented in Fig. 1. The design consists of an array of fingers of width  $40 \, \mu m$ , separation of  $60 \, \mu m$ , and height of  $2 \, \mu m$ . Two working electrodes (first and third from the left on schematics of Fig. 1) attached to IDEAs are used

<sup>&</sup>lt;sup>1</sup>Corresponding author.

Contributed by the Manufacturing Engineering Division of ASME for publication in the JOURNAL OF MICRO- AND NANO-MANUFACTURING. Manuscript received October 29, 2019; final manuscript received February 1, 2020; published online March 27, 2020. Editor: Nicholas Fang.

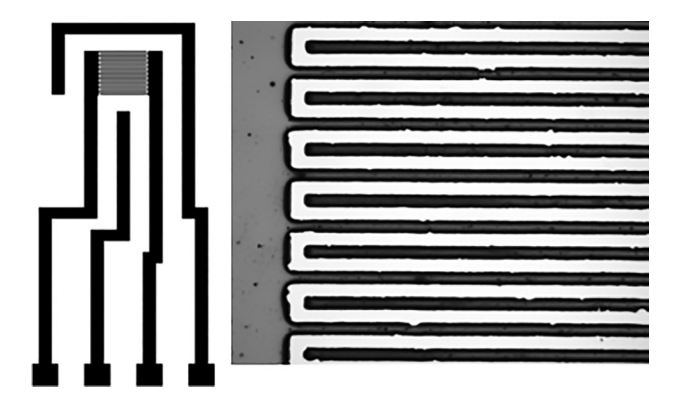


Fig. 1 Schematic drawing of electrode with interdigitated design (left). Micrograph of the IDEAs (right) used in the experiments. The width of the electrode is 40  $\mu$ m.

in this work, whereas the reference electrode and counter electrode (second and fourth from the left on schematics in Fig. 1) are not utilized in the reported studies as these electrodes are designed to be used in electrochemical experiments.

The details of the production of glassy carbon interdigitated electrodes have been published previously [6]. Briefly, the sequence of steps involves lithographic patterning of SU-8 resist and subsequent placing of the wafer with the remaining developed SU-8 in the furnace at elevated temperature under nitrogen environment. After the purge with nitrogen at room temperature for 1 h at 0.5 SCFH, the temperature was ramped at the rate of 25 °C/min, and then the temperature was held at 300 °C for 30 min. The temperature was further increased at the rate of 12 °C/min to

 $900\,^{\circ}\text{C}$  and the held at  $900\,^{\circ}\text{C}$  for 1 h followed by overnight passive cooling to room temperature. After the pyrolysis step, the wafer was diced with a diamond point scribe into individual chips-containing IDEAs.

**2.2 Experimental Setup.** The copper wires were soldered onto the carbon contact pads with indium metal. The wires were then connected to the Function Generator DS345 (Stanford Research Systems, Sunnyvale, CA) to apply the desired AC frequency, offset (V), and voltage (V). Solutions of nonionized carboxylated polystyrene microbeads of 1 and  $5\,\mu\rm m$  in diameter (Magsphere Inc., Pasadena, CA) suspended in the de-ionized water were pipetted onto the interdigitated electrodes and covered by the microscope glass slide to reduce evaporation and facilitate the observation of the movement of the beads. An Eclipse LV-UDM Universal Design Microscope (Nikon Instruments Inc., Melville, NY) was utilized to observe the electrokinetic phenomena.

## 3 Simulation

COMSOL MULTIPHYSICS 5.3a (COMSOL, Inc., Burlington, MA) platform was used to analyze the distribution of electric field that influences the movement of particles.

The electrode geometry studied in this work is a single SU-8-derived glassy carbon electrode pair that is a part of the IDEA. This single electrode finger has a width of  $40\,\mu\text{m}$ , a length of  $2000\,\mu\text{m}$ , and a  $60\,\mu\text{m}$  edge-to-edge separation with adjacent electrodes.

Our hypothesis for the movement of the beads along the length of the electrodes rests on the fact that due to high resistance nature of the electrodes (such as those made of glassy carbon), there is a

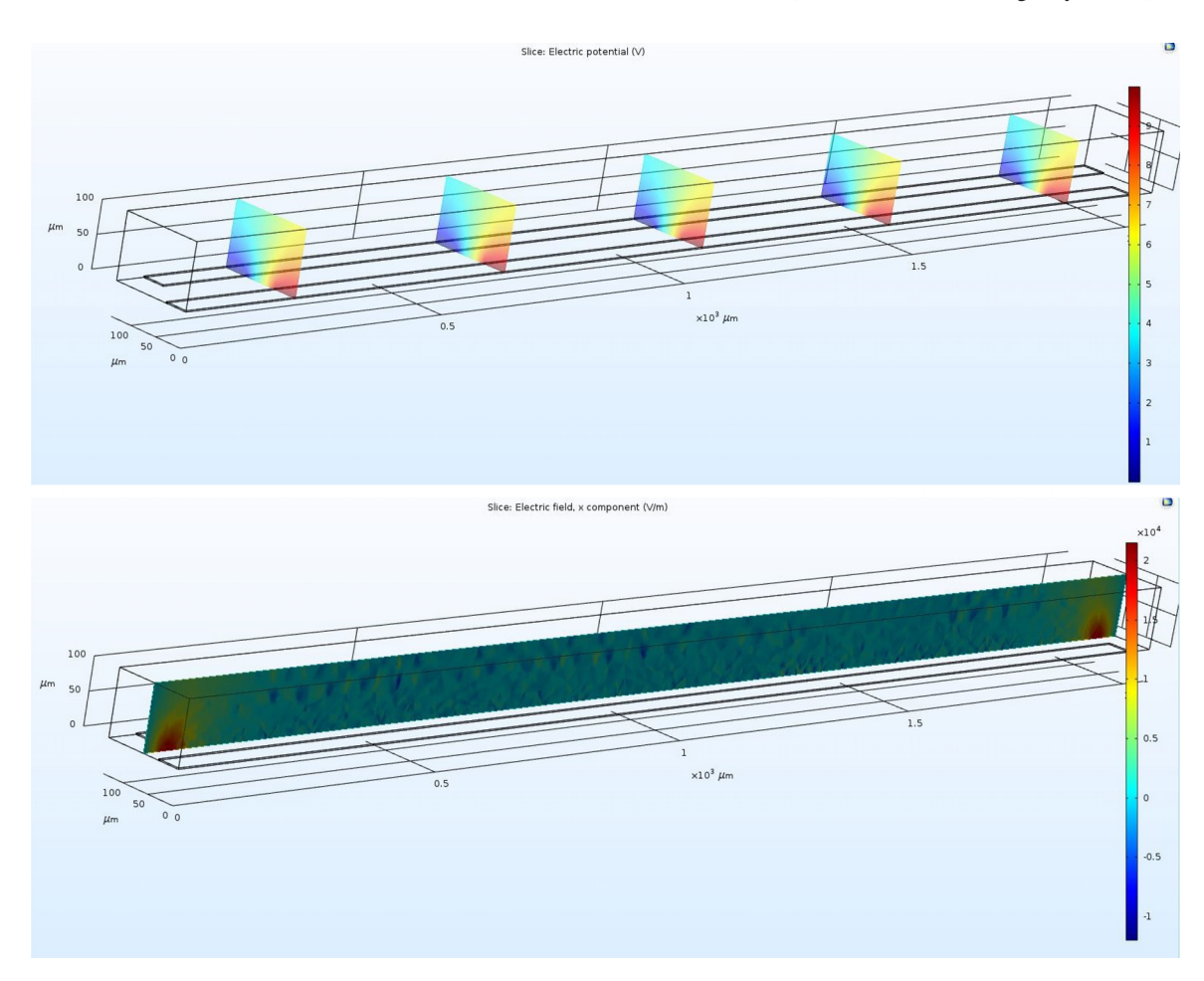


Fig. 2 COMSOL simulation of potential distribution (top) and electric field distribution (bottom) of the IDEA

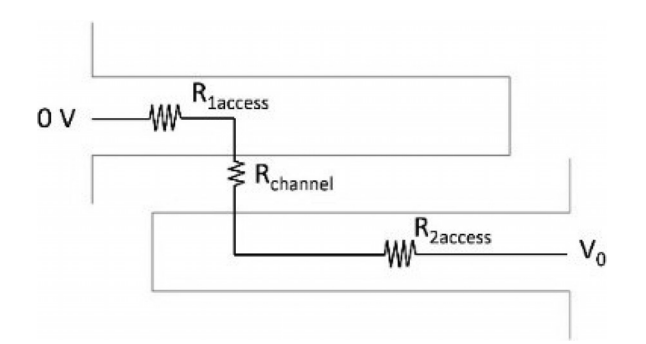


Fig. 3 Electrical schematics representing the resistances of the sections of carbon electrodes (access resistances) and of the resistance of the liquid channel between the electrodes. One electrode is grounded and another electrode has the applied potential  $V_0$ .

potential distribution along the length of the electrodes (i.e., potential is higher at the base of the electrode and falls due to resistive losses as one gets closer to the tip of the electrode). Therefore, electric field and, consequently, electric field gradient changes along the length of the high-resistance electrode in contract to low-resistance electrode (such as those made out of gold or copper) where the potential will stay constant. Thus, we expect that the phenomenon of DEP propulsion along the length of the electrode will not be present for gold IDEAs, but will be present for glassy carbon IDEAs.

The electric potential distribution and the electric field distribution represented in Fig. 2 was simulated for 10 V peak-to-peak (V pp) bias with one electrode having 0 V potential applied at one end of the finger and the other electrode had 10 V applied at the opposite end. The conductivity of the water solution is 0.05  $\mu\text{S/m}$ , and the resistivity of SU-8-derived glassy carbon electrodes is  $4\times10^{-5}~\Omega\text{-m}$ . The relative electrical permittivity of glassy carbon electrodes and aqueous solution were 30 and 80.3, respectively.

The simulation demonstrates that the high field regions are located at the ends of the electrode arrays. These simulation

results are consistent with the experimental evidence discussed below that the beads would tend to move to these high field areas.

To evaluate if the classical dielectrophoretic phenomena (i.e., transverse movement of the beads toward or away from the adjacent electrodes) depend on the location along the length of the high resistance electrode, we used the conformational transformation (mapping) method [7,8] to calculate the voltage drop (the effective voltage difference  $V_{\rm eff}$ ) between the adjacent carbon electrode fingers as presented on plot in Fig. 4. It is suggested that the channel between the fingers of the electrodes acts as a voltage divider as represented by the electrical circuit schematics of Fig. 3. The voltage difference can be calculated according to the following equation:

$$V_{\text{eff}} = V_0 \frac{R_{\text{channel}}}{R_{\text{channel}} + R_{\text{1access}} + R_{\text{2access}}}$$
(3)

In Eq. (3),  $V_0$  represents the voltage applied to the electrodes.  $R_{\rm 1access}$  and  $R_{\rm 2access}$  are the resistances of the segments of two fingers of the interdigitated electrodes, and  $R_{\rm channel}$  is the main channel resistance of the liquid between the adjacent electrodes.

It is evident from the electrical schematics in Fig. 3 that as one moves along the length of the electrodes, whereas individual resistances  $R_{\rm 1access}$  and  $R_{\rm 2access}$  are changing, their sum is staying constant. Therefore, it is evident from Eq. (3) that the effective voltage between the electrode fingers (and thus the electric field) will stay constant regardless the specific location along the length of the electrode (Fig. 4). This is consistent with the finite element analysis comsol simulation results presented in Fig. 2. The sharp increase in electric field is near the tip of the electrode due to abrupt change in geometry, whereas along the length of the electrode the field stays constant.

We can analyze also the dependence of the effective voltage on the distance between the electrodes and the conductivity of the fluid (and thus resistance of the fluid channel).

To calculate the resistances of the segments of carbon electrodes  $R_{1
m access}$  and  $R_{2
m access}$  Eq. (4) is used

$$R_{\rm access} = \frac{\rho L}{A} \tag{4}$$

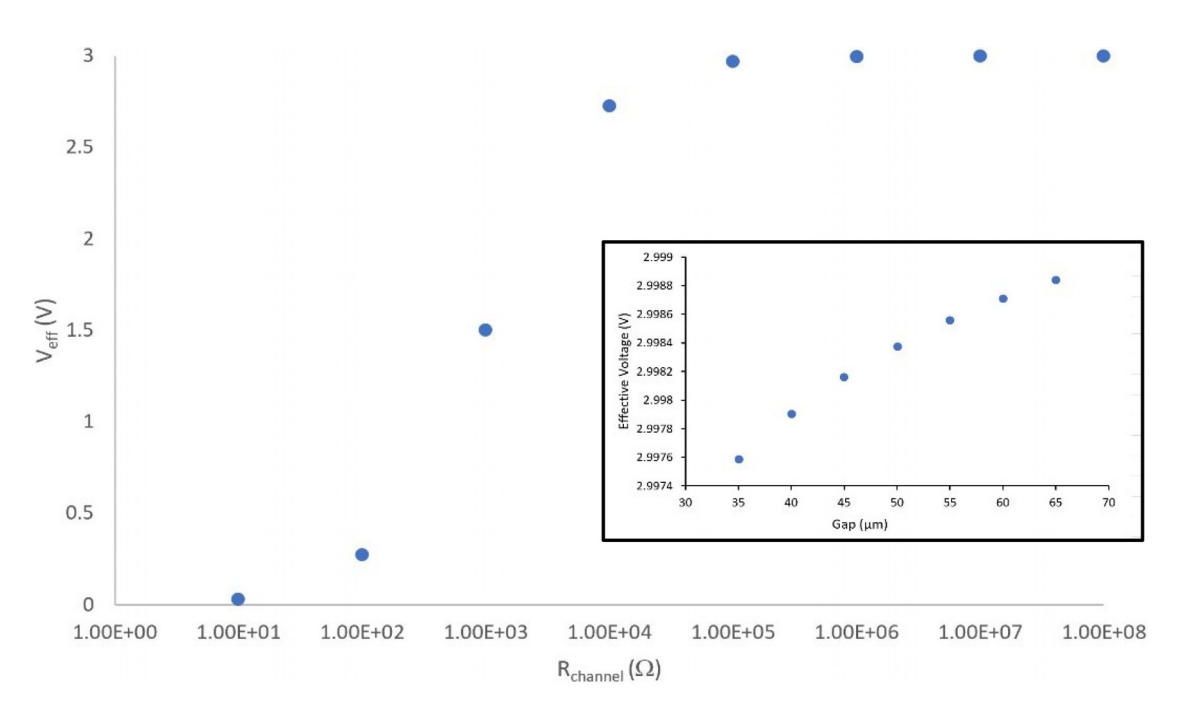


Fig. 4 The graph of effective voltage as function of resistance *R* of the channel when the applied voltage is 3 V peak-to-peak (pp). The inset presents the graph of the effective voltage as function of the gap width between the electrodes.

Table 1 Experimental observation of latex microbeads movement at various applied voltage and frequencies

Diameter of the latex beads ( $\mu$ m)	Applied voltage (V pp)	DC offset (V)	Frequency (kHz)	Observations
1	3	0	<300	Attraction to adjacent electrodes, pDEP, no lateral movement along electrodes
1	3	0	>500	Repulsion from adjacent electrodes, nDEP, no lateral movement along electrodes
5	3	0	<400	Attraction to adjacent electrodes, pDEP, no lateral movement along electrodes
5	3	0	>500	Repulsion from adjacent electrodes, nDEP, no lateral movement along electrodes
1	3	+1.3	100	Repulsion from adjacent electrodes, nDEP, beads move to the left along the electrodes (velocity $\approx 2 \mu m/s$ )
1	3	-1.3	100	Repulsion from adjacent electrodes, nDEP, beads move to the right along the electrodes (velocity $\approx 2 \mu m/s$ )
1	3	-1.1	100	Repulsion from adjacent electrodes, nDEP, beads move to the right along the electrodes (velocity $\approx 1 \ \mu m/s$ )
1	3	-1.0	100	Repulsion from adjacent electrodes, nDEP, beads don't move along the electrodes
Mix of 1 and 5 $\mu$ m beads	3	+1.0	10	About 1 $\mu$ m beads experience attraction toward the adjacent electrodes (pDEP), while 5 $\mu$ m beads are repelled from the adjacent electrodes (nDEP) and move along the electrodes to the left (velocity $\sim$ 17 $\mu$ m/s)

In Eq. (4),  $\rho$  is the resistivity of the glassy carbon  $(4\times10^{-5}\,\Omega\cdot\mathrm{m})$ . L and A denote the length and area of the electrode finger, respectively. If we take a point half-way along the length of the electrode (i.e.,  $1000\,\mu\mathrm{m}$  away from the tip of the electrode), then  $R_{1\mathrm{access}}$  and  $R_{2\mathrm{access}}$  will both be approximately equal to  $500\,\Omega$ .

To calculate  $R_{\text{channel}}$ , the conformal transformation [7,8] is used to obtain

$$R_{\text{channel}} = \frac{4K(k^2)}{\sigma_{\text{m}}h\,k(1-k^2)}\tag{5}$$

In Eq. (5),  $\sigma_{\rm m}$  represents the conductivity of the medium and h is the height of the electrode finger.  $K(k^2)$  is called the complete elliptic integral of the first kind which can be calculated as follows.

$$K(k^2) = \int_{t=0}^{1} \frac{dt}{\sqrt{(1-t^2)(1-k^2t^2)}}$$
 (6)

In Eq. (6), the variable function of K, known as modulus k, is related to the shapes and dimensions of the electrodes. The variable t represents the time.

Modulus k in Eqs. (5) and (6) depends on the geometry of the electrodes. For an electrode configuration with more than two fingers, the definition of the modulus k becomes

$$k = \cos\left(\frac{\pi}{2} \frac{w}{w+s}\right) \tag{7}$$

where w is the width of the electrodes and s is the size of the gaps between the electrodes.

For our specific electrode configuration k is approximately equal to 0.31 and thus K(k) (Eq. (6)) is calculated to be 1.61 and thus the channel resistance from Eq. (5) is approximately equal to 229 T $\Omega$ . Therefore, for glassy carbon electrodes we do not expect that the classical dielectrophoretic behavior in the transverse direction (to or away from the electrodes) will not be affected by the high resistance of the electrodes as the channel resistance exceeds the electrode resistance by many orders of magnitude.

#### 4 Results and Discussion

The set of experiments were conducted under constant amplitude and frequency with a varying offset to examine the phenomenon of DEP propulsion toward the ends of the microelectrode arrays. The offset represents a direct current (DC) shift of the applied bias. Introduction of the offset changes the physics of DEP forces significantly [3,9] and while a particle experiences a positive DEP at zero offset, if nonzero DC offset is applied, particle might experience a negative DEP at the same applied frequency. No validated theory of AC DEP with DC offset has been developed to date. Therefore, we are presenting a phenomenological study based on the experimentally observed behavior of the latex microbeads under several applied AC signals with specific DC offsets. The results of the experiments are summarized in Table 1

When the offset is equal to zero, sinusoidal signal is symmetrical (half of the cycle is positive bias and half of the cycle—negative bias) and such AC DEP force is well described by Eq. (2). When the CM factor is positive, the beads are attracted to the electrode fingers, typically, the increase in frequency will make CM factor negative for simple spherical beads, leading to negative DEP and repulsion of the beads from the electrodes [4]. The crossover frequency of CM = 0 was determined for 1- and 5- $\mu$ m diameter beads to be 0.3–0.5 and 0.4–0.5 MHz, respectively.

Therefore, for zero offset, we observe AC DEP and, depending on the frequency, we see either attraction toward the electrodes or repulsion from neighboring electrode fingers as was reported earlier [6].

If a significant offset is applied, the bias is either mostly, or wholly positive or negative and thus we observe either wholly DC DEP or a mix of AC and DC DEP, depending on the value of the offset. It was discovered that the direction of the bead movement could be manipulated by change in the offset value.

While the details of the physical framework that underlying mixed mode DC/AC DEP is not well understood, results of the several experiments will serve to illustrate the range of possibilities of particle manipulation on the interdigitated carbon electrode microarray when frequency, bias, as well as the DC offset can be varied.

For example, Fig. 5 presents captured frames from the experiment where at the solution of  $1 \mu m$  diameter beads under the

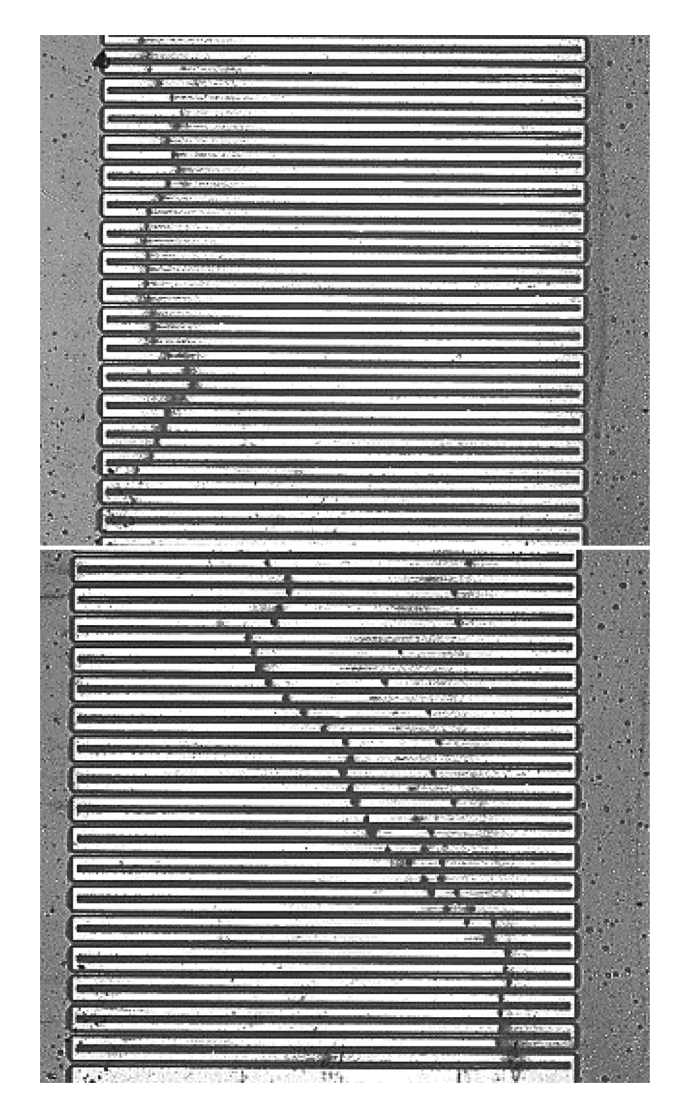


Fig. 5 About 1- $\mu$ m beads under the influence of 100 kHz, 3 V pp bias move to the left edge of the electrode array when the offset is +1.3 V (top), but movement of the beads switches to that toward the right edge when the offset is changed to -1.3 V pp (bottom)

amplitude of  $3\,\mathrm{V}$  pp and  $100\,\mathrm{kHz}$ , and the positive offset of  $+1.3\,\mathrm{V}$  can be seen moving to the left end of the electrode array. When the offset was switched to  $-1.3\,\mathrm{V}$ , the direction of movement changed, and the beads started moving toward the right side under of the electrode array. Thus, a controlled propulsion and movement of the beads toward the regions of high electric field could be achieved successfully by offset manipulation.

Additionally, DEP propulsion can be coupled with positive or negative DEP for the integrated separation of microparticles (such as different subpopulations of biological cells). For example, we have successfully achieved a separation of the mixed solution of 1 and 5  $\mu$ m diameter beads into two groups of beads based on the respective diameter.

Figure 6 demonstrates the sequence of frames captured 2 s apart where the mixed population of beads was separated as at  $10\,\mathrm{kHz}$  and  $3\,\mathrm{V}$  pp, the 1- $\mu$ m diameter beads experienced positive DEP and were attracted to the electrodes, whereas 5- $\mu$ m diameter beads experienced negative DEP and repelled from the electrodes (they can be seen between the electrodes). At the same time, 1-V offset was applied, and 5- $\mu$ m beads moved to the left side of the electrode array. Subsequently, these beads could be collected and removed to a separate location if the goal of the process is the separation step only. However, the separation and propulsion



Fig. 6 The mix of 1 and  $5\,\mu m$  diameter beads is separated under the influence of 10 kHz,  $3\,V$  pp,  $1\,V$  offset bias. The images (top and bottom) were captured  $2\,s$  apart. Smaller beads experience pDEP and are attracted to the electrode fingers (seen as small protrusions along the edges of the electrodes), whereas larger beads move to the left side of microelectrode array. The red oval outlines and the blue rectangular outlines surround several groups of beads on sequential pictures to facilitate identification of the movement of these beads.

combined can be utilized in microassembly to separate out one type of microcomponents and then propel them to a desired location, or in medical diagnostic platforms such as separating and analyzing circulating tumor cells.

# 5 Conclusions

A novel DEP-based propulsion technique utilizing high-resistance electrodes and combining the applied AC signal and DC offset has been described. The simulation describes field distribution within the system confirmed our results of particle moving toward high field at the end of the electrodes. The proof-of-principle operation of separation of 1- and 5- $\mu$ m beads from the mix that integrated separation and propulsion steps has been demonstrated. More phenomenological studies in conjunction with the development of physical framework describing the role of DC offset in charge polarization on dielectric particles is needed to further advance the electrokinetic sorting and propulsion outlined in this study.

## **Funding Data**

- National Science Foundation (Grant No. CMMI-1661877; Funder ID: 10.13039/100000001).
- University of California, Irvine's Undergraduate Research Opportunity Program (UCIUROP) (Funder ID: 10.13039/ 100008476).

#### References

- [1] Cecil, J., Kumar, M. B. R., Lu, Y., and Basallali, V., 2016, "A Review of Micro-Devices Assembly Techniques and Technology," Int. J. Adv. Manuf. Technol., 83(9–12), pp. 1569–1581.
- [2] Van Brussel, H., Peirs, J., Reynaerts, D., Delchambre, A., Reinhart, G., Roth, N., Weck, M., and Zussman, E., 2000, "Assembly of Microsystems," CIRP Ann. Manuf. Technol., 49(2), pp. 451–472.

- [3] Lewpiriyawong, N., Yang, C., and Lam, Y. C., 2012, "Electrokinetically Driven
- [5] Lewphryawong, N., Tang, C., and Lain, T. C., 2012. Electrometerary Brief.
  Concentration of Particles and Cells by Dielectrophoresis With DC-Offset AC Electric Field," Microfluid. Nanofluid., 12(5), pp. 723–733.
  [4] Ramos, A., Morgan, H., Green, N. G., and Castellanos, A., 1998, "AC Electrokinetics: A Review of Forces in Microelectrode Structures," J. Phys. D: Appl. Phys., **31**(18), pp. 2338–2353.
- [5] Hossan, M. R., Dutta, D., Islam, N., and Dutta, P., 2018, "Electric Field Driven Pumping in Microfluidic Device," Electrophoresis, 39(5-6), pp. 702–731.
  [6] Cheng, C. I., Cortez, J., Dorantes, I. B. C., Rodriguez, E. A., Jr., Zad, S. H., and Kulinsky, L., 2018, "The Study of Particle-Particle Interaction and Assembly Under the Influence of Dielectrophoretic Force Experienced Between Carbon Microelectrodes," Proceedings of the World Congress of Micro- and
- NanoManufacturing, Portoroz, Slovenia, Portoroz, Slovenia, Sept. 18-20, Paper

- NanoManufacturing, Portoroz, Slovenia, Portoroz, Slovenia, Sept. 18–20, Paper No. WCMNM-2018-51.
  [7] Demierre, N., Braschler, T., Linderholm, P., Seger, U., Van Lintel, H., and Renaud, P., 2007, "Characterization and Optimization of Liquid Electrodes for Lateral Dielectrophoresis," Lab Chip, 7(3), pp. 355–365.
  [8] Olthuis, W., Streekstra, W., and Bergveld, P., 1995, "Theoretical and Experimental Determination of Cell Constants of Planar-Interdigitated Electrolyte Conductivity Sensors," Sens. Actuators, B, 24(1–3), pp. 252–256.
  [9] Zellner, P., Shake, T., Hosseini, Y., Nakidde, D., Riquelme, M. V., Sahari, A., Pruden, A., Behkam, B., and Agah, M., 2015, "3D Insulator-Based Dielectrophoresis Using DC-Biased, AC Electric Fields for Selective Bacterial Trapping," Electrophoresis, 36(2), pp. 277–283. Electrophoresis, 36(2), pp. 277–283.